J. Biochem. 2011;149(5):601–607 doi:10.1093/jb/mvr019

JB THE JOURNAL OF BIOCHEMISTRY

Melting of DNA–actinomycin clusters

Received September 30, 2010; accepted January 17, 2011; published online February 15, 2011

Nikolai Vekshin*

Institute of Cell Biophysics of Russian Academy of Sciences, Pushchino, Moscow Region, 142290, Russia

*Nikolai Vekshin, Institute of Cell Biophysics of Russian Academy of Sciences, Pushchino, Moscow Region, 142290, Russia. Tel: +8 27 73 94 32, Fax: +0967 33 0509, email: nvekshin@rambler.ru

Differential methods of scanning micro-calorimetry and UV spectrophotometry were used for understanding the interaction of natural anti-tumour antibiotic actinomycin D with cluster sites of native and fragmented DNA during thermal melting. At low (micro-molar) concentrations, the actinomycin molecules penetrate into unwound regions of DNA, but not into the double helix. Moreover, they stabilize the fragmented DNA and increase a total melting point. Actinomycin D interacts with fractions of native DNA even at very low concentrations (at the antibiotic/nucleotide ratio of 1 : 868) and stabilizes the most loose clusters. At high concentrations, it destabilizes the double helix.

Keywords: actinomycin D/calorimetry/DNA clusters/hyperchromism/melting.

Abbreviations: AMD, actinomycin D; 7AAMD, 7-amino-actinomycin D; *h*, hyperchromism.

Powerful anti-microbial and anti-cancer chromopeptides are widely used in medical practice as drugs. A big group of such natural antibiotics are actinomycins. At very low concentrations, they block the mitotic activity of cells, without affecting the basic metabolic processes (*1*). A typical representative of them is actinomycin D (AMD), consisted of a flat phenoxazone chromophore (4,6-dimethyl-2-amino-phenoxazone-3-one-1,9-dicarboxylic acid) and two identical pentapeptides, two amino groups of which are acetylated by two carboxyl groups of the chromophore. The basis of the biological effect of AMD is its ability to form specific complexes with DNA that leads to block the RNA-polymerase reaction, resulting in inhibited protein biosynthesis and cell division (*1*).

There were two opposing models on the formation of DNA–actinomycin complexes. According to the first (*2*), the complex formation is due to embedding of the chromophore and the peptide part of the molecule in the small groove of the double helix of DNA, where AMD is held mainly through hydrogen bonds. This model of surface binding does not take into account the fact that the decisive role in formation of such complexes belongs to hydrophobic interactions (*3*). In particular, the model is not consistent with the fact that spectral properties of the chromophore of the antibiotic in the complex with DNA are identical to those in pyridine, but not in polar solvents (*3*). However, this model correctly emphasizes the fact that the classical rigid double helix is not able to connect AMD anywhere else except on the surface.

The second model—stacking intercalation—means the introducing of the phenoxazone chromophore by stacking type between guanine, cytosine and the adjacent base pair (*4*). Peptide groups thus should be immersed in a small groove. X-ray data are in favour of this model (*5*, *6*). According to X-ray analysis, the presence of guanine, donating the NH_2-group, is necessarily providing to binding. However, oligonucleotides (*7*, *8*) and clusters of guanine (*9*) in aqueous solutions do not show any specificity of AMD to guanine. The antibiotic binds well with many nucleotide sequences (i.e. they may not be necessarily enriched with GC) and even not in double helix (*7–12*). It should be emphasized also that, in contrast to the typical stacking intercalating dye ethidium bromide, which is a potent carcinogen, the AMD, *vice versa*, is an anti-cancer drug.

The reason of the contradiction probably lies in the fact that different researchers used different methods, each of which has its own limits of applicability and requires special conditions. For example, NMR is dealing with milli-molar concentrations, and X-ray analysis with crystals. Structural data obtained by NMR for concentrated solutions and X-ray analysis for the condensed anhydrous phase cannot be automatically extrapolated to the dilute solutions and low concentrations (without appropriate checks by other methods, more sensitive). It should be noted that the physiological effect of AMD is manifested at low (micro-molar) concentrations; but at higher concentrations, the antibiotic is strongly toxic for all cells of human body.

Most researchers proceeded from the premise that AMD has to communicate namely with classical double helix. However, the number of binding sites for molecules of AMD in native thymus DNA is very few [not more than 5 per 100 bp (*1*)]. Almost the same ratio was obtained in the case of fluorescent analog of AMD—7-amino-actinomycin D (7AAMD) during its binding into the DNA of phage lambda (*13*). Maximum binding constant of actinomycins with DNA varies from 10^5 to $10^6\,M^{-1}$ (*13*, *14*), depending on the type of DNA and conditions of incubation in the solution. The binding constant of actinomycins in the case of oligonucleotides is sufficiently higher (*7–14*). The constant is especially high for synthetic

single-stranded hairpins, consisted of three dozen nucleotides, forming a loop (*12*, *13*). Hence, we can assume that actinomycins at low concentrations are incorporated into the hairpin-like areas of DNA—loops and untwisted sites, *i.e.* where there is no classical double helix.

Using absorption spectroscopy (UV, IR and visible region) and fluorescence spectroscopy (steady-state, polarization and phase-modulation), a fundamental difference in complexes of actinomycin with dissolved DNA and condensed film DNA has been demonstrated (*15*). It was concluded that the structure of the AMD–DNA complex in aqueous solution differs from that in the condensed phase. The stacking intercalation of actinomycin between nucleotides was observed only in their film. In solutions of DNA or oligonucleotides, the embedding of actinomycin at its low concentrations occurs without stacking—in small cavities, formed by loops, untwisted sites and hairpins (*9*, *13*, *15*).

The aim of this work is to validate the model of non-stacking binding of AMD into DNA by UV photometry and differential scanning micro-calorimetry, using the heat melting of cluster complexes of DNA–AMD [IR spectroscopy, spectrofluorimetry, stopped-flow and other methods were applied in previous works (*3*, *9*, *13–15*)]. It is known (*16*) that even single point mutations change the melting temperature of DNA (it was found in the denaturing gradient gel capillary electrophoresis). When the AMD–DNA complex is heated, which should lead to any more or less significant features in the melting of different clusters of sites (even when low concentrations of antibiotic are applied).

Experimental Procedures

DNA

Commercial preparations of native DNA from calf thymus (Serva, Germany) were used in all experiments. DNA was dissolved in the 10 mM cacodylate buffer or 5–10 mM phosphate buffer, at neutral pH. The DNA concentration was determined by UV-photometry, based on the extinction coefficient of native DNA $\varepsilon_{260} = 6600\,M^{-1}cm^{-1}$. Usually, a batch of 5 mg of DNA was taken and dissolved in 5 ml of the buffer for 7 h. Next, the absorption spectrum of the diluted aliquot of DNA from the 'mother' solution in the same buffer was recorded on spectrophotometer Specord M-40 (Germany) in the range of 240–320 nm. The purity of DNA was determined by comparing the optical densities at A_{260} and A_{280} in the buffer. Commercial preparations of native DNA are characterized by $A_{260}/A_{280} = 1.885$. To get a fragmented DNA, the uterine DNA solution (1 mg/ml) was ultra-voice treated by an ultrasonic disperser UZDN (frequency was 44 kHz, power was 50 MW) within 5 min. To prevent overheating, the ultrasonic treatment was done on ice, using successive 1-min exposures, followed by 1-min cooling. During this procedure, too long strands of DNA were broken, but there was no denaturation or multiple breaks.

Chemicals

Sodium phosphate (chemically pure), sodium cacodilate (Sigma, USA), AMDand 7AAMD (Reanal, Hungary and Fluka, Switzerland) were used. All solutions were prepared, using distilled water, directly at the day of the experiment. In the experiments, a bittern AMD solution of the 1.27-mM concentration was used. The concentration of AMD was determined photo-metrically, based on $\varepsilon_{440} = 24500\,M^{-1}cm^{-1}$.

Preparation of the DNA–AMD complexes

An aliquot of DNA solution was mixed with AMD solution in the eppendorf test tube, and the obtained volume was adjusted to 1 ml by phosphate buffer. Thus, appropriate concentrations of AMD and DNA at a given molar ratio were prepared. After mixing, the samples were incubated for 3 h at 20°C in a thermostat. To find out whether DNA aggregates (precipitates) or not at a high AMD: DNA ratio, the 2-ml samples were prepared, incubated, and then, 1 ml was centrifuged at 12000*g*, and then the absorption spectra and thermograms of the initial liquor (non-precipitated) and centrifuged samples were compared. All samples passed this test. In our experiments, the micro-molar AMD concentrations did not cause any aggregation and precipitation of DNA.

The DNA melting

Melting of DNA was measured photometrically (by hyperchromic effect in the UV region) and micro-calorimetrically. To test the degree of solubility of the DNA solution, the 1.5-ml volume was placed in an eppendorf tube and precipitated at 12000*g* by the Eppendorf-5414 centrifuge, and again, the concentration was checked UV-photometrically and micro-calorimetrically. In the case of complete dissolution of DNA, it was not scattering in values of A_{260}, enthalpy and intensity of heat absorption.

Micro-calorimetry

The temperature dependence of excess specific heat absorption (hereinafter—the thermogram) of a stock solution of DNA was recorded using the differential adiabatic scanning micro-calorimeter DASM-4 (SKB BP, Pushchino) with platinum-cell volume of 0.5 ml. The device working principle and basic characteristics of DASM-4 were described in (*17*). Thermograms of solutions of DNA with AMD were recorded using the differential adiabatic scanning micro-calorimeter SCAL-1 (Institute of Protein Research, Pushchino) in glass cells of the 0.32-ml volume. The device working principle and basic characteristics of SCAL-1 were described in (*18*). All measurements were performed in the 5 mM phosphate buffer at a rate of heating of 1°C /min and excessive external pressure of 2.5 bar. The noise of DASM-4 does not exceed 350 μJ/°C; the reproducibility of the baseline was not worse than 0.9 μJ/°C. The noise in SCAL-1 does not exceed 15 μJ/°C; the reproducibility of the baseline was not worse than 60 μJ/°C.

Sequence in micro-calorimetric experiments

(i) First stage comprises a sequence of entry of two baselines of the AMD solution at a concentration, corresponding to the concentration of AMD in the presence of DNA. The aim was to make sure that there is no thermo-chemical process (at a given concentration of AMD in the measuring cell), leading to release or absorption of heat. (ii) Second stage includes a consistent recording of two or more baselines of the AMD solution (at a concentration, corresponding to the concentration of AMD in a solution with DNA) during re-filling of both calorimeter cells. It should be emphasized that the micro-calorimetric study of DNA solutions with AMD at the low concentration was possible only because of the micro-calorimeter SCAL-1, equipped with glass cells. In the case of DASM-4, equipped with a platinum mesh, the registration of heat absorption of DNA–actinomycin complexes was impossible because of the thermo-chemical conversion of AMD on the surface of platinum. (iii) Third stage was the recording of heat absorption of the sample. After incubation, the sample was placed in the measuring cell of the micro-calorimeter. After the SCAL-1 goes into the warm-up (to 10°C), the temperature dependence of excess of molar heat absorption was recorded. (iv) Analysis of thermograms was performed using MicroCal™ Origin™ 6 (Microcal Software, Inc., Northampton, MA, USA). Calculations of parameters of heat absorption of DNA were carried out according to (*19*, *20*). To 'extract' the molar heat absorption value of the sample from thermograms, the baseline was subtracted, and then, the area was normalized to the concentration of the sample of an area of electrical calibration of the device. All changes in molar enthalpy (ΔH_{cal}) were determined after subtracting the straight line, connecting the start point and the end of the heat absorption. The intensities of transitions were defined as the movement of heat capacity (ΔC_p^{max}) at the maximum peak of heat absorption at the corresponding temperature maximum (T_{max}). The half-width ($\Delta T_{1/2}$) of transitions was determined as the width of

the entire circuit of heat absorption at half ΔC_p^{max} of the highest A-peak.

UV photometry

The melting of DNA was detected on Specord M-40 by the hyperchromic effect at 260 nm. The value of hyperchromism was found as h (%) = 100 $(A_1-A_0)/A_1$. The raising of temperature in a closed thermostatic quartz cell was carried out in most experiments at a speed of not more than 1°C/min. The measuring cell was placed in a special thermostatically controlled shirt from plexiglas and secured close to the window in the front of the detector. Integral temperature in the cell during the DNA melting was recorded with the accuracy of 0.1°C by semiconductor micro-detector MT4.

Results and Discussion

Hyperchromic effect at melting of fragmented DNA with AMD

Thermal melting of both native and fragmented DNA is accompanied by hyperchromic effect of the band at 260 nm. This effect is associated with disruption of nucleotide stacking leading to decrease in competition of chromophores for photon within the chromophore stack (*21*). This effect is also present in DNA–AMD complexes with micro-molar concentrations of the latter, but its hyperchromism level (h) decreases considerably with increase of AMD:DNA ratio (Table I).

Figure 1 shows UV-photometric melting curves of 'fragmented' thymus DNA during heating from 20°C to 85°C at different AMD concentrations. Fragmented DNA is not too rigid two-stranded helix in the solution at a low ionic strength, easily destroyed at a strong heating. Since at the temperature above 90°C, the hydrolysis of phosphor-diester bonds takes place and additional increase in absorption arises, then the point 90°C shall be regarded as the upper limit of measurements.

Curves in Fig. 1 are upstanding one above the other mainly by means of optical density contribution at 260 nm of AMD itself. The intrinsic absorption of AMD itself raised the baseline of the absorption spectra even at 20°C but this bottom-up does not diminish the degree of the hyperchromic effect, because the hyperchromic value was calculated as the difference between final optical density and initial one in the presence of AMD, and the baseline was subtracted in 'both' curves.

It is hardly possible to determine this contribution quantitatively, since phenoxazone chromophore forms stable bonds with DNA chromophores, accompanied by significant redistribution of electronic density, which changes form of the absorption spectrum and the extinction coefficient intensity not only in the visible region, but also in UV (*3*, *13*). There are two reasons of decrease in the hyperchromic effect of DNA in the presence of AMD: (i) antibiotic induces local disruption of the stacking in DNA at the moment of fixation to it and, therefore, melting curve 'starts' from 20°C at a certain level of a partly hyperchromized DNA, (ii) antibiotic protects (at some small degree) a number of sites in DNA from thermal denaturation. When low concentrations of AMD are used, the second reason is more dominant.

Unlike interaction of AMD with hairpin oligonucleotides (*8*, *11*), where formation of the complex is accompanied by a significant (by 10–15°C) increase of melting temperature T_m, interaction of AMD with fragmented thymus DNA leads only to a small increase of T_m (Table I)—not >1°C or 3°C, when AMD:DNA ratio = 1 : 20 or 1 : 10. At a higher concentration of antibiotic (1 : 5), T_m of the fragmented DNA increases by 5°C.

It shall be noted that effect of AMD in relation to increase in melting temperature is smallish in comparison with effect of salt; melting temperature in tonic solutions, e.g. in the presence of 200 mM sodium chloride, is ~20°C higher than without salt. DNA is known to be not a full rigid double helix in salt-free solutions (*22*), it is partly destabilized and therefore melts more easily than in salt solutions.

Table I. Parameters of melting of DNA found from the hyperchromic effect, at different concentrations of AMD.

DNA	T_{max} (°C)	h (%)
Fragmented, in cacodylate buffer	72 ± 0.7	68.6
In the presence of 2.5 μM AMD	72.9 ± 0.7	55.1
In the presence of 5 μM AMD	74.8 ± 0.7	28.2
In the presence of 10 μM AMD	76.7 ± 0.7	10.1
Native, in phosphate buffer	75.4 ± 0.3	79.5
In the presence of 2.5 μM AMD	76.5 ± 0.3	46.5
In the presence of 5 μM AMD	75.9 ± 0.4	36.9

DNA was 50 μM (of nucleotides); the h-value was measured after a slow melt upon reaching 85°C.

Hyperchromic effect at melting of native DNA with AMD

Melting of 'native' thymus DNA with AMD gives similar picture, but with some significant variances (Fig. 2).

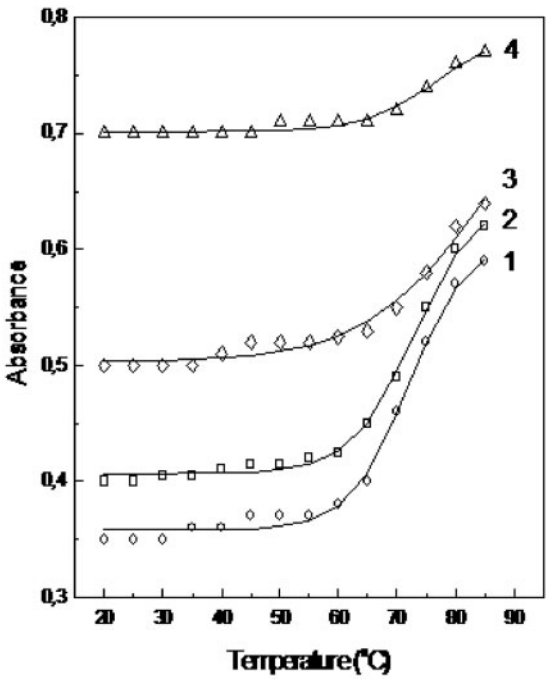

Fig. 1 Melting of fragmented DNA (50 μM nucleotides) in Na-cacodylate buffer at pH 7. (1) DNA (2) DNA in the presence of 2.5 μM AMD, (3) DNA in the presence of 5 μM AMD, (4) DNA in the presence of 10 μM AMD. Optical density was measured at 260 nm.

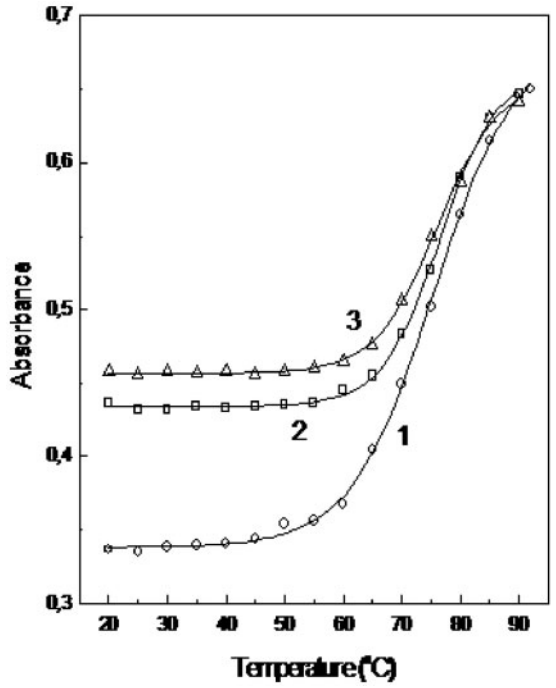

Fig. 2 The melting of native DNA (50 μM nucleotides) in 10 mM Na-phosphate buffer at pH 7. (1) DNA (2) DNA in the presence of 2.5 μM AMD, (3) DNA in the presence of 5 μM AMD. Measurements were done at 260 nm.

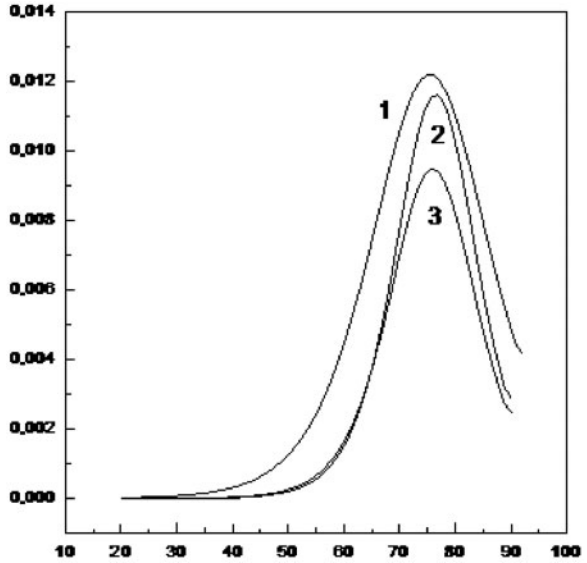

Fig. 3 The first derivative (dA/dT) of melting of native DNA (50 μM bases). (1) DNA (2) DNA in the presence of 2.5 μM AMD, (3) DNA in the presence of 5 μM AMD.

First, other initial level of optical density of the complex is observed. Second, there is other relationship between AMD concentration and *h*. Third, final *h* value changes (Table I). Here, large hyperchromic effect is associated with both larger orderliness of native DNA in comparison with the fragmented one and different exposure of AMD on them.

Interaction of AMD with native DNA leads only to insignificant increase in T_m (Table I)—no more than 1 degree (the accuracy of measurements was 0.3 degree), when AMD:DNA ratio = 1 : 10 or 1 : 20. This means that antibiotic influences a total stability of sites in native DNA only at insignificant degree. Native DNA is much more stable than the fragmented one; it has a higher T_m (Table I). It is difficult for antibiotic to enhance a rather high stability of native DNA at all. Moreover, at higher concentrations, AMD disrupts double helix and T_m starts decreasing.

Only a certain 'mean' melting temperature T_m characterizing the sample in general is detected on the measured UV-photometric curves. More interesting information is obtained after differentiation of the curves. Figure 3 shows differential curves of melting optical density variance dA/dT (first-order derivative) of native DNA and its complexes with AMD. Comparison of the obtained differential curves shows that antibiotic interacts mainly with those DNA regions which melt over the range of 40–70°, but not with a main pool of regions, melting at 70–80°. This expressly suggests that antibiotic is embedded not into a dense double helix (which starts melting intensely at ~75° in our conditions) at micro-molar concentrations, but into a bit unwound regions (melting at far lower temperatures). While binding in such regions, AMD changes their structure, decreases inter-nucleotide stacking, whereupon a certain hyperchromic effect arises. Increase in optical density at 260 nm in response to addition of antibiotic is triggered not only by its contribution to the absorption, but also by induced hyperchromic effect of DNA regions. The same is evidenced by the fact that increase in optical density at 260 nm in case of native DNA was considerably higher than in case of a fragmented one, with the same AMD : DNA ratio = 1 : 20.

Interestingly, during formation of AMD complex with hairpin oligonucleotides a 'hypochromic' effect at the 260-nm band is observed by contrast (*13*). When AMD is bound inside the 'cavity' in such hairpin, it induces its conformational transition from the state of flexible chain (with randomly oriented nucleotides) to a more compact rigid structure, where a certain stacking of nucleotides develops (meanwhile, AMD itself is not stacked with nucleotides). This coincides with the data (*8*, *11*) on increase of thermal stability of hairpin nucleotides in the presence of AMD.

Cluster hyperchromism of DNA at different temperatures

In the above experiments, slow heating of DNA to a high temperature was produced, *i.e.* gradual process of denaturation of DNA occurs in a very wide temperature range, barely noticeable originating with ~40°C and sharply increases with ~75°C. Generally speaking, the process of denaturation of any of the biopolymer is a function of not only temperature but also time. The influence of non-equilibrium of experiments on the thermal denaturation and renaturation (during calorimetry) was shown in (*23*), in particular, the importance of the rate of heating was highlighted and several thermodynamic assessment formulas that yield kinetic information were invited. Traditional thermodynamic description of the melting process eliminates from

consideration of the time as a parameter. This approximation is legitimate only when the dependence of denaturation during the time (at a given temperature) is much slower than most of the temperature (during the experiment). The resulting melting curves depend on the rate of heating. For example, reducing the rate of heating of DNA samples in our experiments from 1 to 0.5 degree/min led to some shift of curves to the right direction and an increase in T_m of ~2°C. One can assume that just varies in the rate of heating, used by different researchers, is one of the reasons for discrepancies T_m of the same objects.

Foregoing it is clear from experiments with a fixed temperature. If the sample is heated quickly (e.g. from 20°C to 85°C in just 3 min) and kept at the final temperature, one can see that the value of hyperchromic effect depends on the desired final temperature (Table II). Each of the melting curves at a given temperature is characterized by not only its T_m, but also its h value. This fact suggests that native DNA contains extensive cluster sites, which melted almost independently of the other sites. Roughly speaking, some clusters melt even at a low temperature (up to 40–70°C), others at a moderate temperature (70–80°C), while others only at a high temperature (80–90°C). This is consistent with calorimetric data on plasmid DNA, according to which the different clusters (nucleotide sequences) melt at strict different temperatures (*24*).

The value of hyperchromic effect (when the temperature reached a final point) depends on the time. That is why the value of h, obtained by a slow melting (at least 65 min) from 20°C to 85°C (Table I) in our experiments, was significantly greater than with rapid heating (3 min, Table II).

When using low concentrations of AMD or 7AAMD, the value of hyperchromic effect at a given temperature decreases (Table II). This suggests stabilization of DNA by antibiotic. At high concentrations of the same antibiotic, on the contrary, hyperchromism increases (Table II). This suggests that high concentrations of the antibiotic starts to break down the double helix.

Clusters at micro-calorimetric melting

Studies of DNA preparations using differential scanning micro-calorimetry, conducted by several authors *(19, 20, 24–30)*, have shown that thermogram is complicated and consists of the main components and four additional peaks (A, B, C and D). Main component belongs to the melting of DNA preparations in general, and additional peaks reflect the melting of satellite DNA fractions (*26*), as well as the fractions of DNA fragments. The satellites show different buoyant density in cesium chloride (*26*). Different DNA sequences have different melting temperature T_{max} of thermogram (*24*, *29*, *30*). For example, the more GC-pairs, the higher T_{max} values (*24*). Contents of GC-pairs in preparations of thymus DNA are as follows: A-peak = 41.6%, B-peak = 49.6%, C-peak = 58% and D-peak = 65%. The influence of ionic strength, concentration and other conditions of equilibrium or disequilibrium melting in micro-calorimetric experiments on DNA was showed and optimal conditions for obtained thermograms, almost independent of the rate of heating, have been shown in Ref. (*28*).

Figure 4 presents the results on the highly sensitive investigation of the influence of AMD on the excess molar heat absorption of solutions of native thymus DNA. Even an extremely small ratio of AMD : DNA, starting with 1 : 868, displays decrease in the intensity of peaks B, C and D. With further increase in the AMD:DNA ratio, all peaks gradually disappear. Only the main component, greatly weakened, is seen. However, the total H_{cal} and the size of cooperative unit

Table II. Hyperhromism of native thymus DNA at various fixed temperatures.

Conditions: (°C)	Initial A_{260}	Final A_{260}	h (%)
72	0.51	0.6	17.6
75	0.51	0.65	27.5
77	0.51	0.68	33.3
85	0.51	0.72	41.2
85 + 1 μM of 7AAMD	0.48	0.63	31.3
85 + 10 μM of AMD	0.55	0.80	45.5

In these experiments, native thymus DNA in 10 mM cacodylate buffer was heated to a final temperature enough quickly (for 3 min).

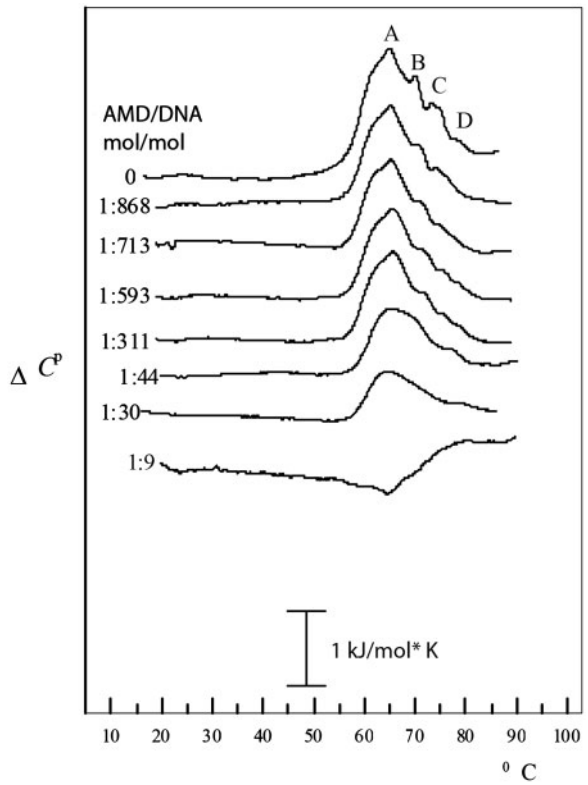

Fig. 4 Effect of AMD on the temperature dependence of excess of molar heat absorption of the solution of native DNA from calf thymus (in 5 mM phosphate buffer, pH 7.4). Thermograms are randomly located one above another. The left of the thermograms indicated the ratio of moles of AMD per mole of DNA nucleotides. Measurements were performed using a differential adiabatic scanning microcalorimeter DASM-4 with platinum-cell volume of 0.5 ml and a differential adiabatic scanning microcalorimeter SCAL-1 with a glass cell volume of 0.32 ml.

N_{melt} do not change, but there is some increase in T_{max} for all peaks (Fig. 5). All these data suggest that AMD effectively interacts with DNA of the satellite fractions and fragments already at very low concentrations (and ratios). With the high ratio (1 : 9) heat absorption characteristic of the native DNA disappears, forming a complex circuit with a peak at 80–90°C, with the other H_{cal}, which exceeds enthalpy of native DNA, and N_{melt} two times smaller than that of the native DNA. It follows from this that with increasing concentration of AMD several completely new thermally stable (but low-cooperative) structures of the complex are formed. The peak of heat absorption at 80–90°C, originating at the ratio of about 1 : 9, is typical [as was shown in (*28*)] for aggregates of denatured DNA. Based on the foregoing, one can conclude that high concentrations of AMD begin to cause denaturation and even aggregation of DNA.

The results of micro-calorimetric melting of the cluster complexes of DNA with AMD are in good agreement with the similar (but obtained with less sensitive calorimeters) data on the interaction of high and medium concentrations of AMD with oligonucleotides and plasmids (*24*) and also with data on the melting of oligonucleotide complexes, containing triplex and duplex motifs and hairpin loops (*31*).

Embedding sites for actinomycins

Interaction of AMD with DNA was once described by a model (*32*) (which became common) that the first molecule of antibiotic associates with arbitrary sequences of the DNA double helix, and then gradually redistributes between the available sites until a thermodynamically optimal binding, *i.e.* AMD reportedly migrates along the double helix to the sites with the highest affinity. This view is contrary to well-known principle of physical chemistry; the most rapid and strong binding should occur in places with a maximum affinity, and only then—in other places. In addition, as shown by the example of 7AAMD using confocal correlation (*14*), polarization and phase (*9*) fluorescence spectroscopy, as well as stop-flow (*13*), a large molecule of the antibiotic binds to DNA immediately, quickly and firmly. The molecule is not capable of appreciable diffusion along the DNA double helix. Kinetics of penetration of AMD in the DNA has two phases: fast (seconds) and slow (minutes) (*13*). Fast phase corresponds to a slight tight consolidation of AMD within unwound, loops and hairpin-like sites, and slow—the difficult penetration of AMD in the double helix.

More detail description of DNA–actinomycin complexes was done recently in a book (*33*).

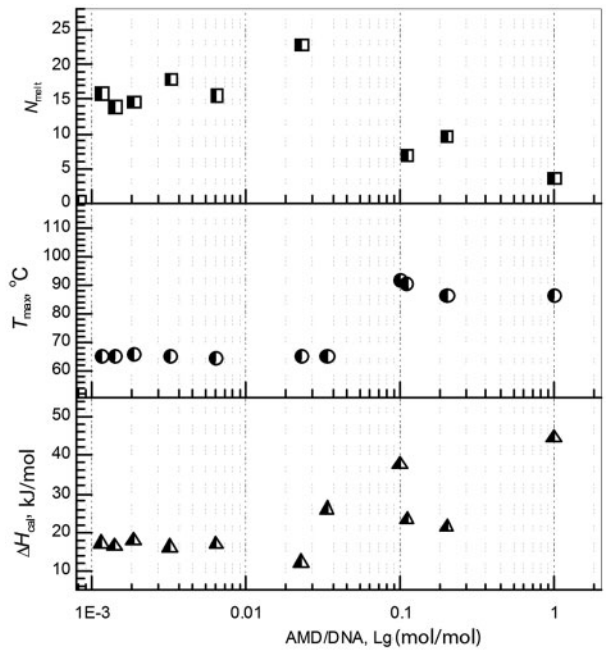

Fig. 5 Influence of various concentrations of AMD on excess of molar heat absorption of DNA.

Conclusions

In this study, highly sensitive methods of differential UV spectrophotometry and differential scanning micro-calorimetry were used for understanding the interaction of small and large quantities of natural anti-tumor antibiotic AMD with clusters of native and fragmented DNA (from calf thymus) during thermal melting. At micro-molar (physiological) concentrations, the actinomycin penetrates in unwound regions of DNA, but not in the double helix. Moreover, it stabilizes DNA and increases the melting point. Antibiotic effectively interacts with nucleotides of native DNA at the ratio of 1 : 868, particularly strongly with clusters of satellite fractions and fragments. At low concentrations, it stabilizes the most loosed clusters that correspond to unwound segments, melted first. At high concentrations, it destabilizes the double helix and causes the aggregation of DNA.

Acknowledgements

The author is grateful to Dr V.R. Akoev, Dr R.E. Elemessov and E.V. Zhilina for participation in preliminary experiments.

Conflict of interest
None declared.

References

1. Egorov, N.S., Silaev, A.B., and Katrukha, G.S. (1987) Actinomycin D in *Antibiotics-Polypeptides* (Egorov, N.S., ed.), pp. 159–204, MGU, Moscow
2. Gursky, G.V. (1969) The structure of complex DNA-actinomycin. *Mol. Biol.* **3**, 749–756
3. Vekshin, N., Savintsev, I., Kovalev, A., Yelemessov, R., and Wadkins, R. (2001) Solvatochromism of the excitation and emission spectra of 7-aminoactinomycin D: implications for drug recognition of DNA secondary structures. *J. Phys. Chem. B* **105**, 8461–8467
4. Muller, W. and Crothers, D.M. (1975) Studies of the binding of actinomycin and related compounds to DNA. *Eur. J. Biochem.* **54**, 267–277
5. Kamitori, S. and Takusagawa, F. (1992) Crystal structure of the 2 : 1 complex between d(GAAGCTTC) and the anticancer drug actinomycin. D. *J. Mol. Biol.* **20**, 445–456

6. Hou, M.H., Robinson, H., Gao, Y.G., and Wang, A.H.J. (2002) Crystal structure of actinomycin D bound to the CTG triplet repeat sequences linked to neurological deseases. *Nucleic Acid Res*. **30**, 4910–4917
7. Snyder, J.G., Hartman, N.G., D'Estantoit, B.L., Kennard, O., Remeta, D., and Breslauer, K.J. (1989) Binding of actinomycin D to DNA: evidence for a non-classical high-affinity binding mode that does not require GpC sites. *Proc. Natl Acad. Sci. USA* **86**, 3968–3972
8. Chen, F.M., Jones, C.M., and Johnson, Q.L. (1993) Dissociation kinetics of actinomycin D from oligonucleotides with hairpin motifs. *Biochemistry* **32**, 5554–5559
9. Savintsev, I.V. and Vekshin, N.L. (2002) Non-stacking binding of 7-amino-actinomycin D and actinomycin D with DNA and model nucleotide systems in solutions. *Mol. Biol*. **36**, 725–730
10. Wadkins, R.M. and Jovin, T.M. (1991) Actinomycin D and 7- aminoactinomycin D binding to single-stranded DNA. *Biochemistry* **30**, 9469–9478
11. Wadkins, R.M., Vladu, B., and Tunng, C. (1998) Actinomycin D binds to metastable hairpins in single-stranded DNA. *Biochemistry* **37**, 11915–11923
12. Wadkins, R.M., Tunng, C., Vallone, P.M., and Benight, A.S. (2000) The role of the loop in binding of an actinomycin D analog to hairpins formed by single-stranded DNA. *Arch. Biochem. Biophys*. **384**, 199–203
13. Vekshin, N. and Kovalev, A. (2006) Prompt non-stacking binding of actinomycin D to hairpin oligonucleotide HP1 and slow redistribution from HP1 to DNA. *J. Biochem*. **140**, 185–191
14. Kovalev, A.E., Yakovenko, A.A., and Vekshin, N.L. (2004) Investigation of 7-amino-actinomycin D and DNA by fluorescence correlated microscopy. *Biofizika* **49**, 1030–1037
15. Savintsev, I.V. and Vekshin, N.L. (2004) Formation of complexes of actinomycins with DNA in solutions and films. *Prikl. Biokchim. Microbiol*. **40**, 421–428
16. Crane, B., Hogan, C., Lerman, L., and Hunter, I.W. (2001) DNA mutation detection via fluorescence imaging in a spatial thermal gradient, capillary electrophoresis system. *Rev. Sci. Instrum*. **72**, 4245–4251
17. Privalov, P.L. and Plotnikov, V.V. (1989) Three generations of scanning micro-calorimeters for liquids. *Thermochim. Acta* **139**, 257–277
18. Senin, A.A., Potekhin, S.A., Tiktopulo, E.I., and Filomonov, V.V. (2000) Differential scanning micro-calorimeter SCAL-1. *J. Therm. Anal. Calorim*. **62**, 153–160
19. Breslauer, K.J. (1995) Extracting thermodynamic data from equilibrium melting curves for oligonucleotide order-disorder transitions. *Methods Enzymol*. **259**, 221–242
20. Duguid, J.G. and Bloomfield, V.A. (1996) Electrostatic effects on the stability of condensed DNA in the presence of divalent cations. *Biophys. J*. **70**, 2838–2846
21. Vekshin, N.L. (2002) *Photonics of Biopolymers*, Springer, Berlin
22. Nakano, S., Fujimoto, M., Hara, H., and Sugimoto, N. (1999) Nucleic acid duplex stability: influence of base composition on cation effect. *Nucleic Acids. Res*. **27**, 2957–2965
23. Potekhin, S.A. and Kovrigin, E.L. (1998) Effect of kinetics factors on heat denaturation and renaturation of biopolymers. *Biofizika* **43**, 198–207
24. Maeda, Y., Nunomura, K., and Ohtsubo, E. (1990) Differential scanning calorimetric study of the effect of intercalators and other kinds of DNA-binding drugs on the stepwise melting of plasmid DNA. *J. Mol. Biol*. **215**, 321–329
25. Mayfield, J.E. (1977) A comparison of the differential DNA melting profiles with the CsCl density profiles of DNA from Escherichia coli, cow, mouse, rat and chicken. *Biochim. Biophys. Acta* **477**, 97–101
26. Melchior, W.B. and Beland, F.A. (1984) Melting of satellite DNA fractions. *Chem. Biol. Interact*. **49**, 177–187
27. Akhrem, A.A., Andrianov, V.T., Vlasov, A.P., Korolev, N.I., and Kuznetsov, I.A. (1985) Micro-calorimetric melting of DNA. *Mol. Biol*. **19**, 623–628
28. Vlasov, A.P., Yakhontova, L.I., and Andrianov, V.T. (1991) Effect of ionic strength, concentrations and other conditions at equilibrium or disequilibrium melting in micro-calorimetry on DNA. *Bifizika* **36**, 437–440
29. Chalikian, T.V., Volker, J., Plum, G.E., and Breslauer, K.J. (1999) A more unified picture for the thermodynamics of nucleic acid duplex melting: a characterization by calorimetric and volumetric techniques. *Proc. Natl Acad. Sci. USA* **96**, 7853–7858
30. Volker, J., Blake, R.D., Delcourt, S.G., and Breslauer, K.J. (1999) High-resolution calorimetric and optical melting profiles of DNA plasmids: resolving contributions from intrinsic melting domains and specifically designed inserts. *Biopolymers* **50**, 303–318
31. Lee, H.T., Khutsishvili, I., and Marky, L.A. (2010) DNA complexes containing joined triplex and duplex motifs. *J. Phys. Chem. B* **114**, 541–548
32. Fox, K.R. and Waring, M.J. (1984) Kinetic evidence for redistribution of actinomycin molecules between potential DNA-binding sites. *Eur. J. Biochem*. **145**, 579–586
33. Vekshin, N.L. (2011) *Biophysics of DNA-Antibiotic Complexes*., Nova Science Publications, NY